Photoelectrochemical property of Fe-N modified titania nanotube array films

LIANQING YU*, LIU RISHAN, YAPING ZHANG, QINGQING WANG, QIANQIAN ZHI, KAITUO DONG
College of Science, China University of Petroleum, Qingdao 266580, P. R. China

In order to fully utilize solar light, highly ordered Fe-N co-doped TiO_2 nanotube array films (NAFs) were fabricated by electrochemical anode oxidation method combined with wet chemical method. The morphology, structure and composition of the as-prepared NAFs were characterized by XRD, SEM and EDX. The concentration of Fe and N on photoelectrochemical property of the TiO_2 NAFs was investigated. The results showed that Fe and N atoms were successfully introduced into the NAFs and enhanced their photoelectrochemical property obviously under solar light. The optimum photoconversion efficiency of 4.83% from light energy to chemistry energy was obtained by preparation in 0.10M/L $Fe(NO_3)_3$.

(Received September 2, 2013; accepted May 15, 2014)

Keyword: Titania nanotube, Fe-N co-doped, Anode oxidation, Photoelectrochemical property, Solar light

1. Introduction

Since highly ordered TiO_2 nanotube array films (NAFs) were reported in 2001 [1], there is great interest in the development of TiO_2 photocatalysis over the past years in fileds of photocatalytic degradation [2-4], solar cell [5-7], gas sensor [8-10], photolysis water [11, 12], etc.. In comparison with nanomaterials dispersed in solution, TiO_2 nanotube array films on Ti foil systems has following virtues: i) more number of electrons transfer between Ti and TiO_2 nanostructures, ii) directly using the film as an electrode, iii) overcoming the obstacle of recycling of TiO_2 particle and iv) absorbing more light due to larger surface area. Fujishima and Honda ever reported [13] that n-type semiconductor TiO_2 was used to split water to obtain hydrogen, because the energy level of TiO_2 matched well with oxidation-reduction potential of water. But until 2006, TiO_2 NAFs of 6μm as light anode, the photoconversion efficiency was still at 0.6% by Grimes [12]. Then, Shankar et al. [14] presented a recent advance toward improving the photoelectrochemical properties of TiO_2 electrodes by structure design.

The relatively wide band gap of TiO_2 limits the efficiency of photocatalytic reactions due to the high recombination rate of photogenerated electrons and holes and the low absorption capability for solar light. Thus, enlargement the absorption band range of TiO_2 NAFs has been considered as an appealing direction for developing the future photo-chemistry.

There have been studies devoted to the improvement of photocatalytic efficiency of TiO_2 nanoparticles, such as doping metal (Fe, Ag, etc.) [10, 15], non-metal (N, C, F, etc.) [16-21]. Transition metal cation doping is generally believed as an effective strategy to reduce electron–hole recombination rate and increase photocatalytical efficiency. In particular, Fe^{3+} is greatly noticed in terms of its semi-full electronic configuration with intermediate energy gap and ion radius close to Ti^{4+} [10]. Also, Xue etc. [21] found that non-metal N can reduce band gap of TiO_2 due to the mixing of p states of N with 2p states of O no matter of replaced N (Ti-N) or clearance N (Ti-N-O). What will happen if the above two mechanisms induced by Fe and N exert a cooperative effect on TiO_2 NAFs? But until now, there is no reports.

In this work, Fe-N co-doped TiO_2 NAFs were prepared by anode oxidation and wet chemical method. The morphologies, structures, photoelectrochemical property of the TiO_2 NAFs were characterized by SEM, XRD, photovoltage and I-V curve.

2. Experimental

2.1 Preparation of TiO_2 NAFs

Titanium foils (10mm×10mm), purity >99.5%, is of 0.20 mm thickness. The graphite electrode (20mm×20mm), purity >99.99%, is of 5 mm thickness. Chemical reagents are all analytical reagent grade quality. The Ti foils were pretreated with acetone, alcohol, deionized water in the ultrasonic bath 15 minutes, respectively. Then the Ti foils were anodized in 0.5M/L NH_4F electrolyte solution under anode voltage of 15-25V with the graphite as counter electrode. The samples of TiO_2 NAFs were calcinated in air ambient at 450^0C for 2h with heating rates of 5^0C/min.

2.2 Preparation of Fe-N co-doped TiO_2 NAFs

The Ti foils were anodized in 0.5M/L NH_4F electrolyte solution containing different concentrations of $Fe(NO_3)_3$ (0.02, 0.05, 0.08, 0.10 and 0.15 M/L) under the

anode voltage of 20V. Then, the TiO_2 films were immersed in 28wt% $NH_3 \cdot H_2O$ with ultrasonic bath 30 minutes, then sealed for 24 hours. Finally, the as-prepared TiO_2 NAFs were calcinated in air ambient at 450^0C for 2h.

2.3 Characterization of the films

The morphologies of NAFs were characterized with a scanning electron microscopy (SEM, model Hitachi S4800, co., Ltd, Japan). Structure of the TiO_2 NAFs after annealing was identified X-Ray Diffractometer (Model Dmax-2700, Dandong Fangyuan instrument, co., ltd., Dandong, China).

2.4 Photoelectrochemical property test

Photoelectrochemical property was tested by using conventional three electrode system: working electrode was TiO_2 NAFs; auxiliary electrode was platinum electrode; reference electrode was Ag/AgCl electrode. The electrolyte solution was 5M/L KOH. Photovoltage and I-V curve was tested by electrochemical workstation (model CHI660B, Shanghai Chenhua instrument co., LTD) under the solar light source (350W xenon lamp). All the experiments were carried out three times.

3. Results and discussions

3.1 Structure analysis

XRD patterns of TiO_2 NAFs are shown in Fig. 1. The diffraction peak of Ti foil appeared obviously at 38.78° and 53.70°, and the diffraction peak appeared at 25.47°, 38.05° , 48.02° , 54.81° and 56.06° corresponding to the (101), (103), (200), (211) and (105) planes of anatase respectively. As $Fe(NO_3)_3$ concentration increase, the peak of (101) planes of anatase enhanced, and obtained the strongest diffraction intensity at 0.1M/L Fe^{3+}. Because of the similar radius of Ti^{4+} (0.0745nm) and Fe^{3+} (0.069nm), it easily leads to the doped Fe^{3+} replacing the Ti^{4+} position in TiO_2 lattice [22]. Moreover, there was no diffraction peak of iron oxide phase observed.

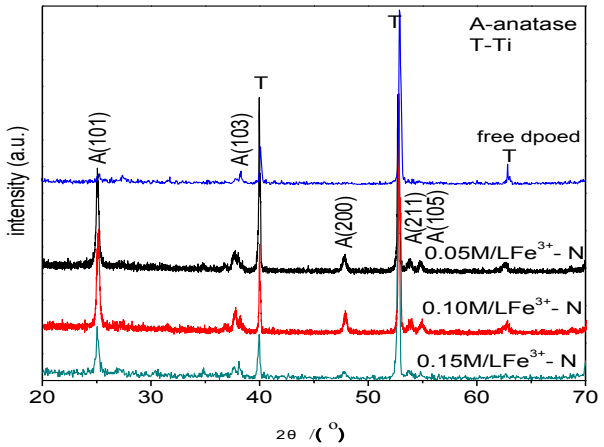

Fig. 1. XRD patterns of TiO_2 NAFs.

The SEM images of TiO_2 NAFs are shown in Fig. 2. For free doped NAFs, the average pore diameter of nanotube is at ca. 100nm and wall thickness at ca. 10nm. The nanotube appears some corrupted arrays and non-uniform morphology with $Fe(NO_3)_3$ solutions of 0.05 M/L and 0.1M/L (Fig. 2b and 2c). When the Fe^{3+} concentration further increased to 0.15 M/L, the nanotube of TiO_2 were totally destroyed and turned into porous structure (Fig. 2d), indicating that Fe^{3+} in the solution can change the NAFs morphology formation. Moreover, there appeared some accumulated nanoparticles on films' surface. The content of Fe increased with Fe^{3+} concentration increase and content of N remained almost constant at ca. 2.0%, measured by EDX (shown in Table 1).

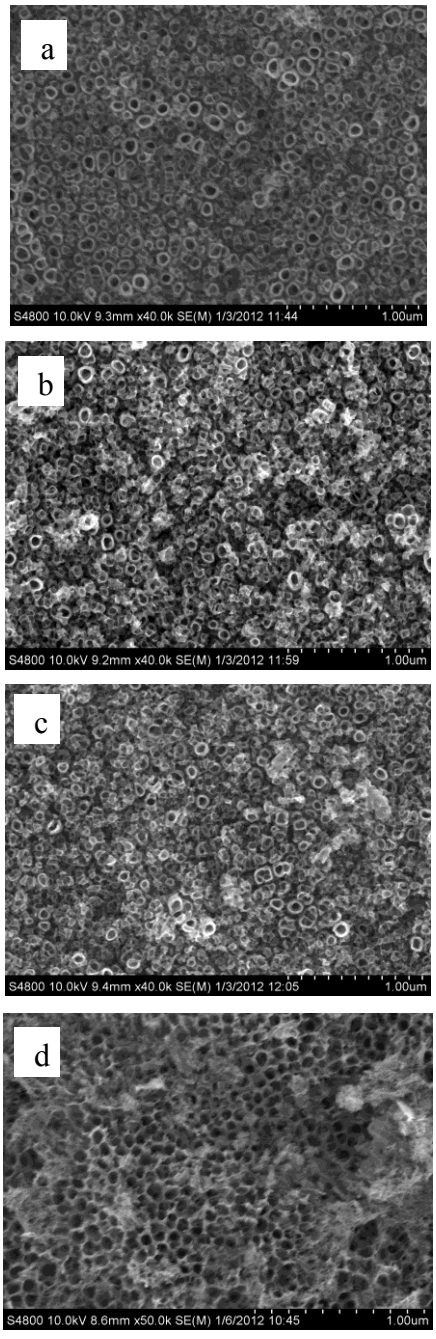

Fig. 2. SEM images of TiO_2 NAFs (a) free doped (b) 0.05M/L Fe^{3+}-N (c) 0.10 M/L Fe^{3+}-N (d) 0.15 M/L Fe^{3+}-N.

Table 1. Properties of TiO_2 NAFs with different preparation technique.

Prepared sample	Element molar content by EDX	Photovoltage (V)	Efficiency (%)	Carrier densities (cm^{-3})
anode voltage 15V	——	0.41	3.0	1.83×10^{19}
anode voltage 20V	——	0.44	3.8	2.51×10^{19}
anode voltage 25V	——	0.38	3.08	2.11×10^{19}
0.10 M/L Fe^{3+}	Fe 4.21%	0.46	3.12	4.04×10^{19}
0.02 M/L Fe^{3+}, N	Fe 0.41%, N 2.10%	0.41	2.6	3.51×10^{19}
0.05 M/L Fe^{3+}, N	Fe 1.86%, N 2.17%	0.35	1.88	1.51×10^{19}
0.08 M/L Fe^{3+}, N	Fe 2.66%, N 2.12%	0.47	2.04	2.12×10^{19}
0.10 M/L Fe^{3+}, N	Fe 4.32%, N 2.16%	0.53	4.83	3.64×10^{21}
0.15 M/L Fe^{3+}, N	Fe 6.23%, N 2.08%	0.21	3.96	1.51×10^{20}

3.2 Photovoltage property

The photovoltage measurements of NAFs are shown in Fig. 3. The nanotube, prepared at anode voltage of 20V, 0.10 M/L Fe^{3+}, N co-doped, owned higher photovoltage value than those of free doped NAFs or solely Fe^{3+} doped, which proved that Fe-N co-doped enhanced the photo-response under solar light. As Fe^{3+} concentration further increased to 0.15 M/L the corresponding photovoltage of NAFs decreased. According to XRD and SEM results in Fig. 1 and 2, the surface morphology and decreased (101) planes of anatase may be account for the decreased photovoltage.

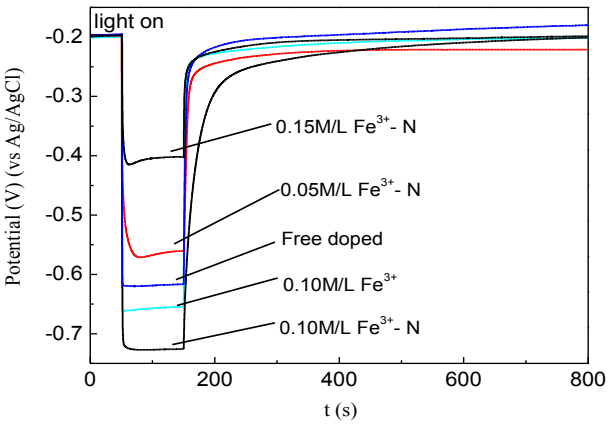

Fig. 3. Photovoltage response of TiO_2 NAFs with different concentration of Fe.

3.3 I-V curve and photoconversion efficiency

I-V curve and corresponding photoconversion efficiency of Fe-N co-doped NAFs are shown in Fig. 4 and Fig. 5. The photoconversion efficiency η is calculated as [23]:

η (%)=[(total power output-electrical power output)/light power input] ×100% =j_p [(E_{rev}^0 - $|E_{app}|$)/I_0] × 100%

where j_p is the photocurrent density (mW/cm^2), $j_pE_{rev}^0$ is the total power output, $j_p|E_{app}|$ is the electrical power input, and I_0 is the power density of incident light (mW/cm^2). E_{rev}^0 is the standard reversible potential which is 1.23V/NHE, and the applied potential is $E_{app}=E_{meas}-E_{aoc}$, where E_{meas} is the electrode potential (vs Ag/AgCl) of the working electrode at which photocurrent was measured under illumination and E_{aoc} is the electrode potential (vs Ag/AgCl) of the same working electrode under open circuit conditions. The voltage at which the photocurrent becomes zero was taken as E_{aoc}.

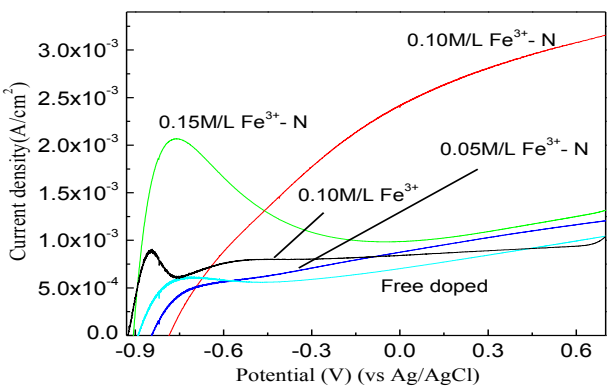

Fig. 4. I-V curve of TiO_2 NAFs under solar light.

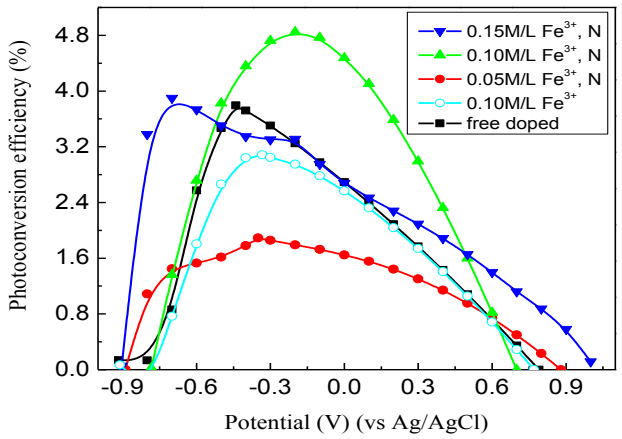

Fig. 5. Photoconversion efficiency of TiO_2 NAFs under solar light.

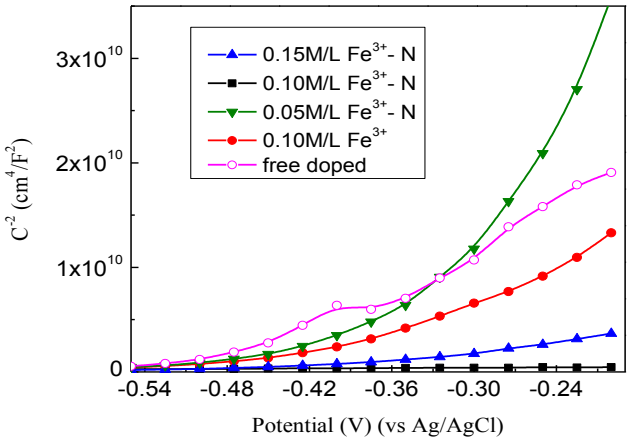

Fig. 6. Mott-Schottky curve of TiO_2 NAFs.

Photoconversion efficiency η of Fe-N co-doped TiO_2 NAFs larger than that of free doped or solely Fe-doped under solar light. The optimum η from light energy to chemical energy is obtained at 4.83%. This enhancement can be ascribed to followings: firstly, the Fe^{3+} doping in the TiO_2 promote the separation of photogenerated electron–hole pairs, but over-doped Fe^{3+} may act as the recombination centers of the electron-hole pairs [23]; secondly, according to density functional theory, either replaced nitrogen (Ti-N) or clearance nitrogen (Ti-N-O) can decrease TiO_2 band gap with 0.12eV or 0.07eV [24], respectively. Therefore, Fe-N co-doped TiO_2 NAFs are benefit for photoelectrochemical property enhancement under solar light.

3.4 Mott-schottky curve

Mott-schottky curve can indicate charge carrier density of semiconductor [25]. In the photoelectric system, light makes system produce an amplified photovoltage, which charged the space-charge capacitance of semiconductor. The charge quantity of space-charge region can influence charge carrier densities (N_D), which is inverse ratio to Mott-schottky curve linear part of the slope. In Mott-Schottky plots, the N_D was calculated using the relation: $N_D = 2/e\varepsilon\varepsilon_0 m$, where e is the elementary electron charge, ε is the dielectric constant (ε=80), ε_0 is the permittivity in vacuum ($\varepsilon_0 = 8.85\times10^{-14}$ F/cm), and m is the slope of the Mott-schottky curves.

The slope of Mott-schottky curve decreases with the increase of Fe^{3+} concentration (Fig. 6), which can be ascribed to N_D increased (Table 1). The N_D of Fe-N co-doped TiO_2 NAFs is higher than free doped or solely Fe^{3+} doped, which proved that Fe-N co-doped can promote the separation of photogenerated electron–hole pairs and absorb more energy from solar light.

4. Conclusions

Fe-N co-doped TiO_2 NAFs were successfully prepared by a facile anode oxidation method. The as-prepared TiO_2 NAFs exhibited excellent photoelectrochemical property under solar light due to greatly increased charge carrier densities. The concentration of Fe^{3+} and N in TiO_2 NAFs played a crucial role on improving the photoelectrochemical property by effective separation of electron–hole pairs and decrease band gap. And the maximum energy conversion from solar light to chemistry was obtained at 4.83%.

Acknowledgement

The financial support by the National Natural Science Foundation of China (No. 20806093), Natural Science Foundation of Shandong Province (No. ZR2011EMQ001), Technology Project of Qingdao 11-2-4-4-(10)-jch, the Fundamental Research Funds for the Central Universities (11CX05013A, 10CX02012A) is gratefully acknowledged.

References

[1] D. Gong, C. A. Grimes, O. K. Varghese, W. C. Hu, R. S. Singh, Z. Chen, E. C. Dickey, J. Mater. Res. **16**, 3331 (2001).
[2] J. M. Macak, M. Zlamal, J. Krysa, P. Schmuki, Small, **3**, 300 (2007).
[3] Y. K. Lai, L. Sun, Y. C. Chen, H. F. Zhuang, C. J. Lin, J. W. Chin, J. Electrochem. Soc., **153**, 123 (2006).
[4] H. F. Zhuang, C. J. Lin, Y. K. Lai, L. Sun, J. Li, Environ. Sci. Technol., **41**, 4735 (2007).
[5] G. K. Mor, K. Shankar, M. Paulose, O. K. Vargheese, C. A. Grimes, Nano Lett., **6**, 215 (2006).
[6] H. Wang, C. T. Yip, K. Y. Cheung, A. B. Djurisic, M. H. Xie, Y. H. Leung, W. K. Chan, Appl. Phys. Lett., **89**, 023508 (2006).

[7] M. Paulose, K. Shankar, O. K. Varghese, G. K. Mor, B. Hardin, C.A. Grimes, Nanotechnology, **17**, 1446 (2006).
[8] O. K. Varghese, D. W. Gong, M. Paulose, K. G. Ong, E. C. Dickey, C. A. Grimes, Adv. Mater., **15**, 624 (2003).
[9] O. K. Varghese, G. K. Mor, C. A. Grimes, M. Paulose, N. Mukherjee, J. Nanosci. Nanotech, 4, 733 (2004).
[10] J. Zhang, Y. P. Zhang, L. Q. Yu, X. L. Zhong, W. X. Wang, Rare Metals, **30**, 267(2011).
[11] O. K. Varghese, M. Paulose, K. Shankar, G. K. Mor, C. A. Grimes, J. Nanosci. Nanotech, **5**, 1158 (2005).
[12] M. Paulose, G. K. Mor, O. K. Varghese, K. Shankar, C. A. Grimes, J. Photochem. Photobiol. A: Chem. **178**, 8 (2006).
[13] A. Fujishima, K. Honda, Nature, **238**, 37 (1972).
[14] K. Shankar, J. I. Basham, N. K. Allam, O. K. Varghese, G. K Mor, X. Feng, M. Paulose, J. A. Seabold, K.S. Choi, C. A. Grimes, J. Phys. Chem. C, **113,** 6327 (2009).
[15] I. Paramasivam, J. M. Macak, A. Ghicov, P. Schmuki, Chem. Phys. Lett. **445**, 233 (2007).
[16] R. Asahi, T. Morikawa, T. Ohwaki, K. Aoki, Y. Taga, Science, 293, 269 (2001).
[17] R. Nakamura, T. Tanaka, Y. Nakato, J. Phys. Chem. B, **108**, 10617 (2004).
[18] L. Q. Yu, K. T. Dong, Y.P. Zhang, Q. Q. Wang, B. Neppolian, Science of Advanced Materials, (2014) in press
[19] Y. H. Ao, J. J. Xu, D. G. Fu, C. W. Yuan, Micropor. Mesopor. Mater. **118**, 382 (2009).
[20] L. Q. Yu, Q. Q. Wang, C G. Liu, Y. P. Zhang, L. Z. Hao, Chemical Engineering & Technology, **37**, 1(2014)
[21] J. J Xu, Y. H. Ao, M. D. Chen, D. G. Fu, Appl. Surf. Sci. **256**, 4397 (2010).
[22] D. F. W. J. Cui, Y. F Gu, X. L Zhang, Journal of Lanzhou University of Technology, **37**, 23 (2011).
[23] S. U. M. Khan, M. Al-Shahry, W. B. Ingler Jr., Science, **297**, 2243 (2002).
[24] L. Mi, Y. Zhang, P. N. Wang, Chem. Phys. Lett., **458**, 341 (2008).
[25] S. E. John, S. K. Mohapatra, M. Misra, Langmuir, **25**, 8240 (2009).

*Corresponding author: iyy2000@163.com